

## Application Note AN M52

# Fourier Transform Vibrational Circular Dichroism FT-VCD Spectroscopy

**M. Urbanova, V. Setnicka, K. Volka**, Institute of Chemical Technology, Technicka 3, 16628 Praha 6, Czech Republic

**B. Jun, D.L. Weaver**, Department of Physics, Tufts University, Medford, MA 02155 USA

**C.P. Schultz**, Bruker Optics, 19 Fortune Drive, Billerica, MA 01821 USA

**M. Boese, H.H. Drewns**, Bruker Optik GmbH, Rudolf-Plank-Str. 27, D-76275 Ettlingen, Germany

### Introduction

Chiral molecules can exist in either of two so-called enantiomeric forms or configurations which are nonsuperimposable mirror images of one another. Chirality means handedness, because right and left hands are not superimposable but each can in principle be created by reflection of the other in a mirror plane. In general, a molecule which in itself does not have a symmetry element (axis, plane) will be chiral. Typically this will occur when a tetrahedral site such as a carbon atom has four different substituents. Such sites are called asymmetric or chiral centers and their configuration is denoted as R or S on the basis of the Cahn-Ingold-Prelog rules. (The older D, L nomenclature for absolute configuration is based on the choice of reference compounds and can be ambiguous). Thus, one of the simplest chiral molecules would be methane with three different substituents (e.g. CHFCIBr), whereby the central carbon represents the chiral center, as shown in Figure 1. More complex molecules such as sugars and steroids may have  $n$  chiral centers, giving  $2^n$  stereoisomers and  $2^{n-1}$  different pairs of mirror-image

enantiomers. For example, for  $n = 2$  the enantiomeric pairs are RR, SS and RS, SR, while RR and RS, for example, are diastereomers and not mirror images. Note that other subtle forms of chirality can occur in molecules without classical asymmetric centers, e.g. octahedral complexes with an appropriate arrangement of ligands, molecules with dissymmetric perpendicular planes or helix-like structures. In general, enantiomers have identical physical properties, except as described below, and give identical UV, IR, and NMR spectra, while diastereomers have similar but distinguishable spectroscopic and chemical properties.

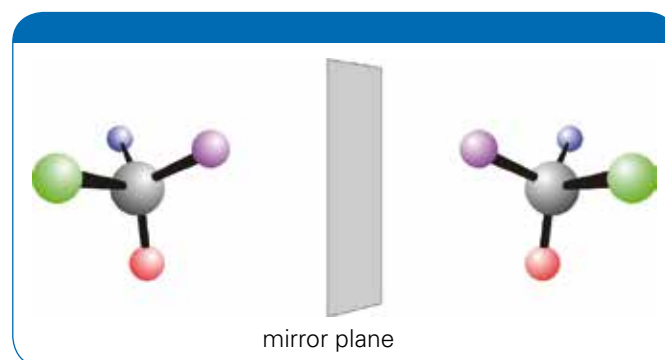


Figure 1: Enantiomers of a tri-substituted methane

Chemists have been aware of chirality or handedness for more than a century since the enantiomers of a given molecule often form distinguishable crystal structures in the solid state or, when in solution, rotate the plane of polarized light equally but in opposite directions. The symbols (+) or (-) placed before a compound's name are used to denote whether a given enantiomer (regardless of its R, S nomenclature) causes at a specified wavelength a clockwise or counterclockwise rotation, respectively. This so-called optical activity or dichroism arises due to differential absorption of left- or right-circularly polarized light, and can be especially useful for elucidating the structures of species which do not easily form crystals.

The interaction between light and a chiral molecule depends on the circular polarization of the probing light. The absorbance  $A_R$  of right-circularly-polarized light by a "right-handed" molecule will be equal to the absorbance  $A_L$  of left-circularly polarized light by the corresponding "left-handed" enantiomer. If the light is probing a symmetric molecule lacking a chiral center or a racemic mixture (equal mixture of the enantiomers), then clearly  $A_L - A_R = 0$ . But so long as there is an excess of one form or the other of a given chiral species, the differential absorption of left-versus right-circularly polarized light  $A_L - A_R$  will not be zero, as shown in Figure 2. The quantity  $\Delta A = A_L - A_R$  depends on the wavelength and is termed the circular dichroism; it represents a measure of the chirality of the probed species and determines the direction and degree of rotation of the plane of linearly polarized light. Note that the sign and magnitude of  $\Delta A$  is determined by the specific orientation and polarizability of the atoms or groups around a chiral center;  $\Delta A$  can be either positive or negative for a given configuration (e.g. (R)- enantiomer) but will always be equal in magnitude and opposite in sign for R vs. S enantiomers.

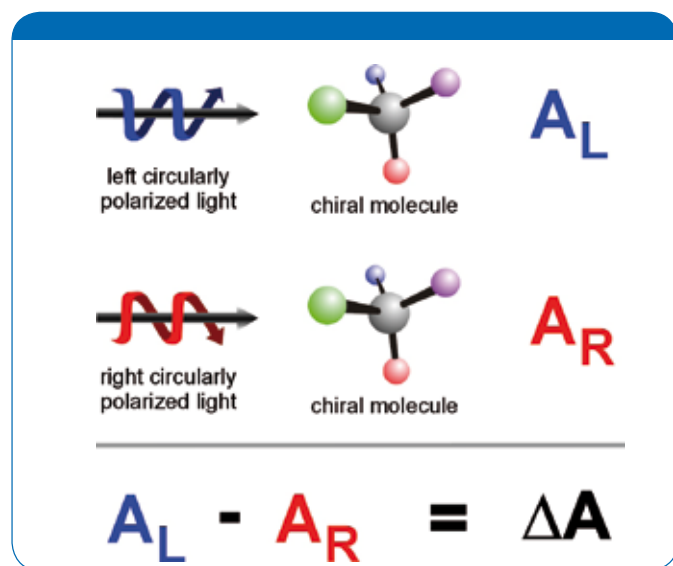


Figure 2: Interaction of chiral molecule with left and right circularly polarized light

The chirality of a molecule not only determines certain physical properties such as crystal structure and dichroism but, more importantly, also its chemical reactivity. Two

molecules must have the appropriate handedness or stereochemistry in order to combine or react. This stereospecificity of reaction mechanisms is of crucial importance in biochemistry where most enzymic reactions require a specific configuration or conformation of the reacting species. Most antibiotics are also involved in stereospecific reactions so that potency is strongly determined by stereochemistry, and only a molecule with the appropriate stereochemistry will exhibit the full range of antibiotic efficiency. Nature assembles most molecules in very specific ways, and the building blocks of the key biopolymers are chiral.

The measurement of Circular Dichroism (CD) as a function of wavelength in the visible and UV regions has been possible with commercial instrumentation for some time, but applications have been somewhat limited. In CD the absorption bands are usually rather broad, and measurements are often limited by the low sample concentrations required (particularly for biomolecules) due to high extinction coefficients and light-scattering effects (the latter are particularly troublesome in the UV/Vis range).

If CD measurements are carried out in the infrared region, the method is termed vibrational circular dichroism or VCD, which is defined as the difference in absorption of a sample for left vs. right circularly polarized infrared radiation  $\Delta A = A_L - A_R$ . VCD has some very distinct advantages: most molecules have significant IR absorption cross sections; sharp IR lines are associated with specific vibrational modes and more structural information can be obtained from a VCD measurement than from a CD spectrum. The Bruker PMA 50 module is especially designed for VCD and for other polarization modulation experiments like PM-IRRAS, and it can be attached to the Bruker TENSOR II, INVENIO and VERTEX series FTIR spectrometers, Figure 3.



Figure 3: PMA 50 attached to a Bruker INVENIO R FTIR spectrometer

VCD spectroscopy can be applied in various ways<sup>1,2</sup>. The VCD signal intensity, that means the difference in the absorption of left and right circularly polarized light, depends linearly on the concentration and path length, just as known from classical IR spectroscopy. The advantage of VCD spectroscopy is that two enantiomers exhibit VCD spectra with the same features but with opposite sign. An equivalent mixture of two enantiomers, a racemic mixture, shows no VCD signal intensities. This behaviour leads to the possibility of the determination of the optical purity, the enantiomeric excess, after an appropriate calibration of the investigated system.

Another application arises from the fact that the two enantiomers have VCD spectra with opposite sign, so they are clearly distinguishable. Often the chemical structure of a substance is well known, but it is not possible to grow a single crystal for X-ray structural analysis, the only absolute method to determine the absolute configuration. Comparing a measured VCD spectrum with an *ab initio* calculated one can be used to determine the absolute structure of a compound with known chemical structure.

Chirality is not limited to the configuration of the atoms in a molecule, as the secondary structure - the 3 D arrangement of large molecules - can be chiral too. Thus it is not astonishing that the VCD spectra of proteins depend on the secondary structure, and VCD spectroscopy can be used to distinguish between the secondary structures of proteins and peptides. The studies of such asymmetric biological molecules<sup>3-7</sup> and their conformational changes<sup>8-12</sup> often associated with protein functionality or enzymatic activity, belong among the most exciting applications of VCD spectroscopy. For these purposes, VCD devices should satisfy the following demands: the measuring system must be very sensitive and stable over time because biological molecules often provide VCD signals at least one order of magnitude weaker than the VCD signals of e.g. terpenes. It is also desirable to measure the VCD spectra of biological molecules in varying physical and chemical conditions. In addition, VCD devices have to be sensitive to a large intensity scale since the intensity of VCD signals can dramatically change because of conformational variations of the biomolecules.

In this application note, the high sensitivity and stability of the Bruker PMA 50 VCD accessory are shown by the VCD measurements of terpenes in the mid-IR region which can be compared to previous measurements<sup>13-16</sup>. The VCD spectra are used for the enantiomeric excess determination. This quantity determination is done by statistical analysis of the VCD spectra of different mixtures of (1R)-(+)- and (1S)-(-)- $\alpha$ -pinene.

As an example for a second application, three different proteins with well known secondary structure are used to demonstrate the dependence of VCD signal on the secondary structure. Hemoglobin, predominantly with an  $\alpha$ -helical structure, concanavalin A, as a protein with predominantly  $\beta$ -sheet secondary structure, and lysozyme, which has nearly the same content of  $\alpha$ -helical and  $\beta$ -sheet structural elements, were chosen<sup>3-7</sup>.

The comparison of the experimental and the calculated VCD spectra leads to a powerful application of VCD spectroscopy, which is demonstrated in the case of (+)-camphor. A very good fit between the theoretical and real data is obtained. This method can be used to determine the absolute structures of compounds<sup>17,18</sup>.

## Experimental

All substances were taken from suppliers and were used without any further purification. The VCD spectra were measured using a Bruker FTIR spectrometer equipped with

the Bruker polarization modulation accessory PMA 50. In the PMA 50 module, the light beam is focused onto the sample passing through an optical lowpass filter (blocking wavenumbers  $>1800\text{cm}^{-1}$ ), a KRS-5 wire grid polarizer, and a ZnSe Photoelastic Modulator "PEM" with an oscillation frequency of 42 kHz. The light is focused by a ZnSe lens to a MCT detector. Figure 4 presents a block diagram of the PMA 50 module in VCD mode.

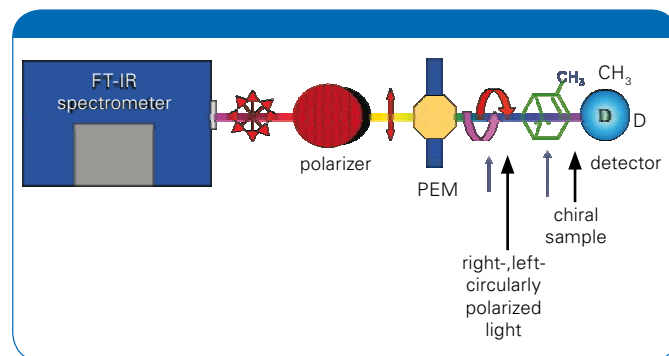


Figure 4: Block diagram of the PMA 50 in VCD setup

The detector signal comprises two components: a low-frequency modulation which corresponds to the IR absorption bands, i.e., the A signal, and a high-frequency modulated signal (42 kHz) corresponding to the dichroic absorptions, i.e., the  $\Delta A$  signal. Additionally, the reference signal direct from the PEM (42 kHz) is mixed to the high-frequency modulated detector signal. These two high-frequency modulated signals are demodulated by an internal synchronous demodulator integrated in the electronic units of the TENSOR II, INVENIO and VERTEX series FTIR spectrometers. The absorption and VCD spectra were measured simultaneously both with resolution of  $4\text{ cm}^{-1}$  in the case of terpenes, and  $8\text{ cm}^{-1}$  in the case of proteins. The VCD spectra were obtained from measured interferograms by applying the dedicated OPUS VCD calculation routine. For each measurement, the intensity calibration factor was obtained using a multiple-wave retardation plate combined with the second wire grid polarizer, whereby the system tuning was exactly the same as for the sample measurement<sup>19</sup>.

**Terpenes:** The liquid samples were placed in a demountable Bruker liquid cell A145 equipped with KBr windows separated by  $50\mu\text{m}$  teflon spacers. In the case of  $\alpha$ -pinene the neat liquid was used, racemic mixtures were prepared volumetrically. The measurements of camphor were carried out in a 3 M  $\text{CCl}_4$  solution.

**Proteins :** The proteins were measured as 5 %  $\text{D}_2\text{O}$  solution in a demountable Bruker liquid cell A145 equipped with  $\text{CaF}_2$  windows separated by  $25\mu\text{m}$  teflon spacers.

## Computation

A major advance in the application of FT-VCD spectroscopy has been realized with the introduction of efficient *ab initio* quantum mechanical computational programs and affordable high-speed computers. With the addition of density functional theory (DFT) methods, a significant improvement in the accuracy of predicted VCD spectra has been achieved

at relatively low computational cost compared to the Hartree-Fock/Self-Consistent Field (SCF) methods previously employed. In a theoretical calculation, the VCD spectrum is obtained by the ratio of two quantities called rotatory strength  $R_{fi}$  and dipole strength  $D_{fi}$ , the latter depending on the electric dipole moment of the molecule and the former on the joint electric and magnetic dipole moments, all evaluated over the molecular basis set. A basis set is the mathematical description of the orbitals within a system (which in turn combine to approximate the total electronic wavefunction) used to perform the theoretical calculation. Larger basis sets more accurately approximate the orbitals by imposing fewer restrictions on the locations of the electrons in space. It is common in ab initio molecular calculations to replace Slater atomic orbitals by functions based on Gaussian functions. Ab initio calculations use basis functions comprising integral powers of  $x$ ,  $y$  and  $z$  multiplied by  $\exp(-\alpha r^2)$ ,  $x^a y^b z^c \exp(-\alpha r^2)$ . This is called a primitive Gaussian function.  $\alpha$  determines the radial extent (or "spread") of a Gaussian function. The order of these Gaussian-type functions is determined by the powers of the Cartesian variables:  $a+b+c$ . The computational methods are used to theoretically calculate the VCD spectrum of a molecule whose experimental VCD spectrum has been measured<sup>17</sup>.

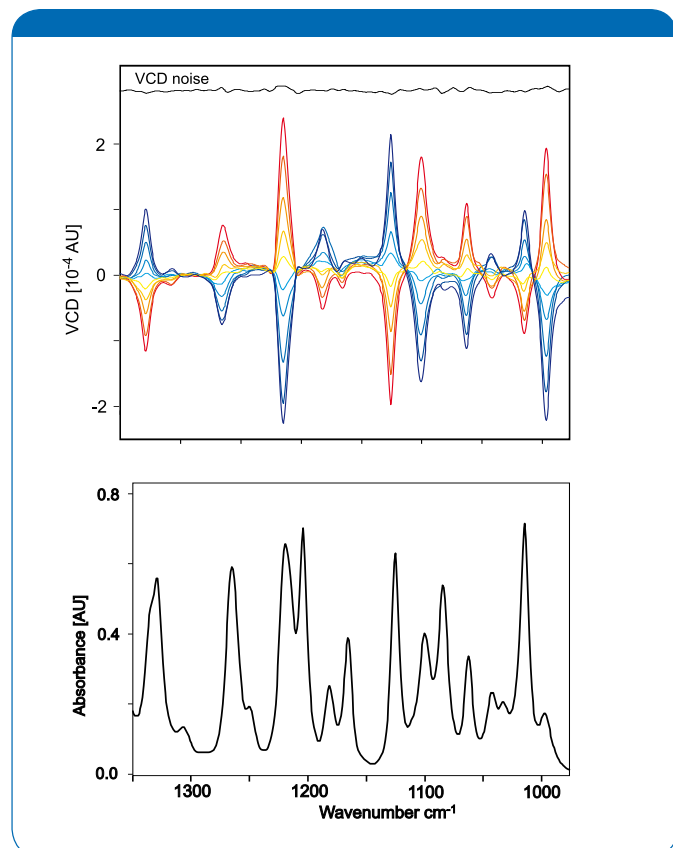


Figure 5: VCD (A) and absorption (B) spectra of (1R)-(+)-pinene and (1S)-(-)- $\alpha$ -pinene with  $f_{ee}$  values of +100, +75, +50, +25, +10, -10, -25, -50, -75, -100% from blue to red. Spectra were collected as the neat liquid in a 50  $\mu$ m KBr cell with a resolution of 4  $\text{cm}^{-1}$

## Results and discussion

Figure 5 presents the absorption and VCD spectra of  $\alpha$ -pinene with different enantiomeric excess. All the samples were measured as a neat liquid. The spectra were obtained as the average of two blocks consisting of 3390 scans. The collection time for each block was 30 min. The VCD spectra were corrected for baseline. The experimental baseline was obtained by the VCD measurement of the racemic mixtures of  $\alpha$ -pinene. The noise spectra were calculated as the half difference between two VCD spectra, which were obtained from consecutive blocks of scans. In the case of the  $\alpha$ -pinene spectrum, the noise level expressed as the root of mean square (RMS) is  $2.8 \times 10^{-6} \Delta A$  unit in the spectral range shown in Figure 5. A powerful analytical application of the VCD spectroscopy is the determination of the optical purity of chiral samples. For this purpose, the optical purity is expressed as the enantiomeric excess<sup>12</sup>  $f_{ee}$ . If the concentrations of (1R)-(+)- $\alpha$ -pinene and (1S)-(-)- $\alpha$ -pinene are  $c_R$  and  $c_S$ , respectively, then the percent enantiomeric excess  $f_{ee}$  is defined<sup>12</sup> as:

$$f_{ee} = \frac{c_R - c_S}{c_R + c_S} \cdot 100 \quad (1)$$

The quantity  $f_{ee}$  is +100% for a sample of the pure (1R)-(+)- $\alpha$ -pinene and -100% for a sample of the pure (1S)-(-)- $\alpha$ -pinene. Ten samples consisting of (1R)-(+)- $\alpha$ -pinene and (1S)-(-)- $\alpha$ -pinene in different concentrations covering the enantiomeric excess  $f_{ee}$  from +100% to -100% were prepared volumetrically. Their absorption and VCD spectra are presented in Figure 5. Absorption spectra of all samples are identical because the standard infrared absorption spectroscopy does not distinguish between the enantiomers, while the optical purity is clearly detected by VCD. The measured VCD spectra of the samples with the different enantiomeric excesses were evaluated by a linear regression. For this purpose, the areas of four bands with maxima at 1329, 1215, 1126 and 996  $\text{cm}^{-1}$ , which roughly cover the whole measured region, were calculated by using the OPUS integration routine. The results show a very good linear correlation between the enantiomeric excess  $f_{ee}$  and the VCD band areas. The correlation coefficients are close to 1 ( $R > 0.998$ ) for all selected bands. The reliability of the results was proved by statistical analysis of the optical purity determination. The regression coefficients and their standard deviations were used for the determination of the four independent values of the enantiomeric excess and their uncertainties for the selected bands. Then their weighted average  $f_{ee}^*$  and standard deviations  $s^*$  were calculated. The standard deviations of  $f_{ee}^*$  (see Figure 6) obtained in this study are  $< 3\%$ . The small standard deviations obtained prove the credibility of the PMA 50 module VCD set up<sup>16</sup>. The uncertainty of the volumetrically determined value of  $f_{ee}$  was also taken into account for a total evaluation of the deviation of  $f_{ee}^*$ . The dependence of the calculated enantiomeric excess  $f_{ee}^*$  and the volumetrically determined enantiomeric excess  $f_{ee}$  is plotted in Figure 6 together with their deviations.

## Biomolecules

In addition to small organic molecules, it is quite easy to obtain VCD spectra of biomolecules such as proteins and nucleic acids. To demonstrate the suitability of this technique for monitoring conformations and conformational changes in biomolecules, we have recorded the VCD and absorption spectra of the proteins hemoglobin, lysozyme and concanavalin A in D<sub>2</sub>O solution (50 mg/ml; 25 μm liquid cell with CaF<sub>2</sub> windows). The spectra were recorded with 8 cm<sup>-1</sup> resolution. The amide I region (primarily the amide C=O stretching) and the amide II region (N-H bending and C-N stretching) are depicted in Figure 7.

These proteins were chosen because of their different secondary structures. Note that all three absorption spectra are very similar, showing a broad featureless absorption in the amide I region. However, these proteins are in fact quite different: hemoglobin is predominantly in α-helix form, concanavalin A is primarily an anti-parallel β-sheet, while lysozyme contains both of these secondary structure elements. We expect that the VCD signal for the amide I band will be sensitive to the secondary structure of the peptide backbone, and Figure 7 demonstrates that the three proteins show distinct VCD spectra and that α-helix and β-sheet motifs give different and specific VCD signals. Thus, FT-VCD spectroscopy is very suitable for charac-

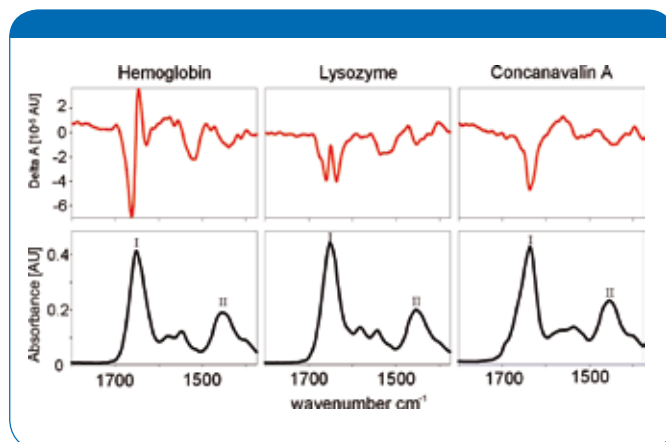


Figure 7: VCD spectra (top) and absorption spectra (bottom) for the amide I and amide II regions of the proteins hemoglobin, lysozyme, and concanavalin A in a 5% D<sub>2</sub>O solution. The amide I band is denoted "I", the amide II band is denoted "II".

terizing the secondary structure of proteins in solution and for monitoring changes in protein conformation caused by ligand binding, for example. In contrast, structure elucidation by X-ray diffraction techniques requires the often difficult production of single crystals with questionable relevance to the solution properties of proteins in the native state.

$f_{ee}$ [%]	$f_{ee}^*$ [%]	$s^*$
100	97.1	2.9
75	77.1	2.7
50	52.5	2.5
25	25.5	2.3
10	9.6	2.2
-10	-11.9	2.1
-25	-27.5	2.2
-50	-47.8	2.4
-75	-76.2	2.6
-100	-98.5	2.8

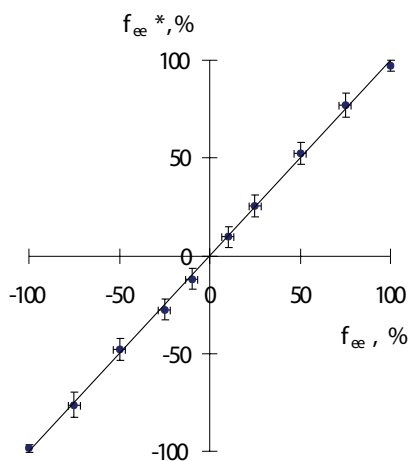


Figure 6: The calculated  $f_{ee}$  and volumetrically determined  $f_{ee}$  values of enantiomeric excess and their standard and experimental deviations.

## Complementary Theoretical Methods

The experimentally measured VCD spectrum of a chiral molecule can for example be compared with the spectra calculated for the two possible enantiomers. Since enantio-

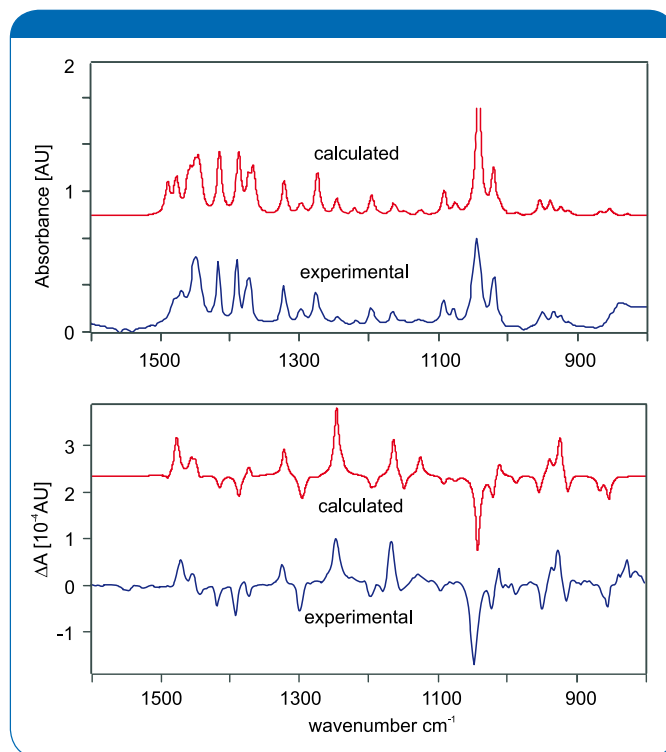


Figure 8: Top: absorbance spectra of (+)-camphor, calculated (red) and measured (blue). Bottom: VCD spectra of (+)-camphor, calculated (red) and measured (blue).

mers produce "mirror-image" VCD spectra of opposite sign, it is generally easy to assign the experimental result to one of the two possible enantiomers. Figure 8 depicts the absorption and VCD spectra of (+)-camphor in a 3 M  $\text{CCl}_4$  solution. The spectra were measured in 30 min at a resolution of  $4\text{ cm}^{-1}$  using a liquid cell with  $\text{BaF}_2$  windows and a path length of  $50\ \mu\text{m}$ . It is clear that computational procedures are now at a level of sophistication where they not only produce

reasonably accurate absorption spectra to confirm a basic molecular structure but can also be used to determine the absolute configuration via the predicted VCD spectrum.

## Summary

Vibrational circular dichroism (VCD) is a relatively easy (and inexpensive) method for measuring the chiral properties of molecules in solution, for determining absolute stereochemical configuration, and for studying the conformational properties of complex biomolecules such as proteins and nucleic acids. The beauty of the technique is that it allows one to determine not only the constitution of a molecule (types of chemical bonds and functional groups), but, particularly when combined with computer modeling techniques, the absolute three-dimensional orientation of the structural elements of a molecule as well.

## References

1. Keiderling, T.A. Vibrational Circular Dichroism: Comparison of Techniques and practical consideration. In Ferraro, J.H., Krishnan, K. (ed.): Practical Fourier transform infrared spectroscopy. Industrial and laboratory chemical analysis. San Diego: Academic, 1990, 203-284; see also Vibrational Circular Dichroism, L.A. Nafie, T.A. Keiderling and P.J. Stephens, J. Am. Chem. Soc. 98, 2715-2723 (1976).
2. Nafie, L.A. Vibrational optical activity. Appl. Spectrosc. 50: 14A-26A, 1996.
3. Freedman, T.B., Nafie, L.A., Keiderling, T.A. Vibrational Optical Activity of Oligopeptides. Biopolymers 37: 265-279, 1995.
4. Pancoška, P., Yasui, S.C., Keiderling, T.A. Enhanced sensitivity to conformation in various proteins. Vibrational circular dichroism results. Biochemistry 28: 5917-5923, 1989.
5. Pancoška, P., Yasui, S.C., Keiderling, T.A. Statistical analyses of the vibrational circular dichroism of selected proteins and relationship to secondary structures. Biochemistry 30: 5089-5103, 1991.
6. Urbanová, M., Dukor, R.K., Pancoška, P., Gupta, V.P., Keiderling, T.A. Comparison of  $\alpha$ -lactalbumin and lysozyme using vibrational circular dichroism. Evidence for difference in crystal and solution structures. Biochemistry 30: 10479-10485, 1991.
7. Keiderling, T.A., Wang, B., Urbanová, M., Pancoška, P., Dukor, R.K. Empirical studies of protein secondary structure with vibrational circular dichroism and related techniques:  $\alpha$ -lactalbumin and lysozyme examples. Faraday Discuss. Chem. Soc. 99: 263-285, 1994.
8. Urbanová, M., Pancoška, P., Keiderling, T.A. Spectroscopic study of the temperature-dependent conformation of glucoamylase. Biochim. Biophys. Acta 1203: 290-294, 1993.
9. Bormett, R.W., Asher, S.A., Larkin, P.J., Gustafson, W.G., Ragunathan, N., Freedman, T.B., Nafie, L.A., Balasubramanian, S., Boxer, S.G., Yu, N.-T., Gersonde, K., Noble, R.W., Springer, B.A., Sligar, S.G. Selective examination of heme protein azide ligand-distal globin interactions by vibrational circular dichroism. J. Am. Chem. Soc. 114: 6864-6867, 1992.
10. Setnicka, V., Urbanová, M., Král, V., Volka, K. Vibrational circular dichroism spectroscopy as a tool for studies of non-covalent interactions between heterocyclic compounds and polypeptides. In Froelich, J. (ed.): The seventeenth congress of heterocyclic chemistry, August 1-6, 1999, Vienna, Institute of Organic Chemistry, Institute of Technology, 1999: PO-110.
11. Bour, P., Záruba, K., Urbanová, M., Setnicka, V., Matejka, P., Fiedler, Z., Král, V., Volka, K. Vibrational circular dichroism of tetraphenylporphyrin. A computational study. Chirality 12: 191-198, 2000.
12. Nafie, L.A., Freedman, T.B. Vibrational circular dichroism: An incisive tool for stereochemical applications. Enantiomer 3: 283-297, 1998.
13. Long, F., Freedman, T.B., Hapanowicz, R., Nafie, L.A. Comparison of step-scan and rapid-scan approaches to the measurement of mid-infrared Fourier transform vibrational circular dichroism. Appl. Spectrosc. 51: 504-507, 1997.
14. Wang, B., Keiderling, T.A. Observations on the measurement of vibrational circular dichroism with rapid-scan and step-scan FT-IR techniques. Appl. Spectrosc. 49: 1347-1355, 1995.
15. Tsankov, D., Eggimann, T., Wieser, H. Alternative design for improved FT-IR/VCD capabilities. Appl. Spectrosc. 49: 132-138, 1995.
16. Urbanova, M., Setnicka, V., Volka, K. Measurement of concentration dependence and enantiomeric purity of terpene solutions as a test of a new commercial VCD spectrometer. Chirality 12, 191-203, 2000.
17. Gaussian 98 (Revision A.1), Gaussian Inc., Pittsburg PA (1998).
18. Devlin, F.J., Stephens, P.J., Cheeseman, J.R., Frisch, M.J. Prediction of Vibrational Circular Dichroism Spectra Using Density Functional Theory: Camphor and Fenchone. J. Am. Chem. Soc. 118: 6327-6328, 1996.
19. Polavarapu, P.L. In: Ferraro, J.R., Basile, L.J., eds. Fourier Transform Infrared Spectroscopy, Vol. 6. New York: Academic Press, 1985: 61.

### ● Bruker Optik GmbH

Ettlingen · Deutschland  
Phone +49 (7243) 504-2000  
Fax +49 (7243) 504-2050  
info.bopt.de@bruker.com

### Bruker Optics Inc.

Billerica, MA · USA  
Phone +1 (978) 439-9899  
Fax +1 (978) 663-9177  
info.bopt.us@bruker.com

### Bruker Shanghai Ltd.

Shanghai · China  
Phone +86 21 51720-890  
Fax +86 21 51720-899  
info.bopt.cn@bruker.com

[www.bruker.com/optics](http://www.bruker.com/optics)

Bruker Optics is continually improving its products and reserves the right to change specifications without notice.  
© 2018 Bruker Optics BOPT-4000359-02